PAN

Opto-Electronics Review

journal homepage: https://journals.pan.pl/opelre

Link range optimisation for detection methods under scintillation effects on FSO system

Sowmyaa Vathsan M S[1], Prakash P[1*], Kasthuri P[1], Sasithradevi A[2]

[1] Department of Electronics Engineering, MIT Campus, Anna University, Chennai, 600044–Tamil Nadu, India
[2] Centre for Advanced Data Science, Vellore Institute of Technology, Chennai, 600127–Tamil Nadu, India

Article info

Article history:
Received 26 Dec. 2024
Received in revised form 22 Apr. 2025
Accepted 30 Apr. 2025
Available on-line 26 May 2025

Keywords:
coherent detection;
free-space optical communication;
optical communication;
quadratic phase shift keying;
scintillation.

Abstract

Free-space optical (FSO) communication is a promising technology that aims to solve the problem of limited bandwidth in modern cellular communication systems. This work investigates the FSO communication systems under varying atmospheric conditions using direct, Mach-Zehnder interferometer (MZI), and coherent detection methods. A detailed analysis evaluates their trade-offs in cost, complexity, and performance. Results indicate that coherent detection achieves the highest link range with an optimal bit error rate (BER) across all turbulence regimes, with maximum feasible ranges of 7.4 km, 6.6 km, and 6.5 km under weak, moderate, and strong scintillation, respectively. Further, optimising local oscillator (LO) power significantly improves system reliability under strong turbulence, enabling robust communication. This study highlights the advantages of coherent detection for FSO systems, particularly in strong scintillation regimes which provide better receiver sensitivity and link range coverage.

1 Introduction

Compared to radio frequency (RF) communication, optical communication improves performance due to a higher frequency carrier wave which ensures faster modulation rates. Free-space optical (FSO) communication transmits visible or infrared light through the atmosphere, offering high-bandwidth optical links [1, 2]. In contrast, optical fibre cable (OFC) networks using OFC cores as a communication channel are becoming increasingly widespread. FSO connections do not necessitate the excavation or installation of any fibre infrastructure. The high installation cost of OFC networks makes them economically unfeasible.

Additionally, relocating fibre-based networks after installation is challenging. FSO communication supports 5G internet access in remote areas due to its simpler deployment and cost-effectiveness compared to optical fibre. The FSO link extends fibre output to connect with another base station [3], addressing the end-mile issue in traditional optical fibre communication. Factors like geometric loss, misalignment loss, pointing loss, scintillation loss, and atmospheric loss degrade signal quality. FSO system reliability is sensitive to varying channel conditions (fog, rain, haze, snow) due to fading and dispersion, with scintillation causing major signal strength fluctuations. To enhance transmission, it is essential to study the channel characteristics for various detection methods.

One such detection method is a direct detection method which involves detecting the modulation of an optical signal without the need for a local oscillator (LO) or energy-consuming digital signal processing [4]. Intensity modulation/direct detection (IM/DD) systems using an on-off keying (OOK) modulation are limited in estimating signal intensity in a scintillating environment where light intensity fluctuations are rapid and random [5, 6]. To improve the receiver sensitivity and suppress the channel fading effect, a differential phase shift keying (DPSK) has been considered. Higher-order DPSK modulation such as differential quadrature phase shift keying (DQPSK), 8-PSK, and 16-PSK provide a 3 dB improvement in the receiver sensitivity to the OOK system and enhance the spectral efficiency [7].

Wang *et al*. [8] demonstrated the statistical analysis of a bit error rate (BER) performance in DPSK, which OOK formats in moderate, as well as strong turbulent channels.

*Corresponding author at: prakashp_mit@annauniv.edu

https://doi.org/10.24425/opelre.2025.154745
1896-3757/ Association of Polish Electrical Engineers (SEP) and Polish Academic of Sciences (PAS). Published by PAS

Jaworski [9] presented a comparison of high-capacity optical modulation formats for high-speed dense wavelength division multiplexing (DWDM) transmission systems, showing the superiority of a DQPSK modulation over other formats, and the use of Manchester coding [10] improved spectral efficiency. Based on the gamma-gamma channel model, the BER expressions for three distinct detection methods [homodyne detection, heterodyne detection, and Mach-Zehnder interferometer (MZI) detection] have been determined by Xie *et al*. [11]. Nasu *et al*. [12] proposed a DQPSK demodulation technique using an MZI-type planar light wave circuit (PLC), achieving high-data rates with minimal error. DQPSK improves spectral efficiency by encoding two bits of information with four optical phase shifts [13].

Coherent detection and digital signal processing enable high-speed, long-distance transmission, reaching up to 400 Gbps in commercial core-metro networks, data centres, and access networks. Coherent optical QPSK systems also support FSO communication, where QPSK modulation offers a higher data rate than binary phase shift keying (BPSK) [14–16]. In this work, the data transmission rate for the FSO system is limited to 10 Gbps to optimise the maximum feasible link range. Direct, MZI, and coherent detection schemes are evaluated under varying scintillation conditions, including weak, moderate, and strong regimes. The proposed approach uses a coherent detection scheme with an optimised LO power to mitigate scintillation effects.

2 Methodology

Figure 1 presents a schematic representation of the fundamental FSO system which consists of three main components: the transmitter section, the channel, and the receiver section.

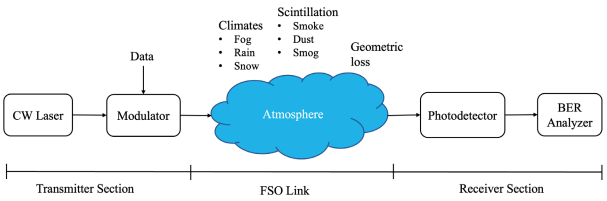

Fig. 1. Basic block of the FSO system with losses in the channel.

Several new innovative techniques have been deployed to improve the performance and capabilities of the receiver section. Overall, these advancements in receiver technology contribute to enhanced optical signal demodulation, increased receiver sensitivity, and reduced power consumption.

2.1 Detection methods

This work examines direct, MZI, and coherent detection methods which offer varying trade-offs in terms of cost, complexity, and performance, and are widely used in FSO systems.

DD is preferred for its simplicity and efficiency in short-range communication, while MZI detection enhances dispersion management for mid-range links. Coherent detection offers superior sensitivity and is well-suited for long-range communication under challenging conditions like strong scintillation.

2.1.1 Direct detection (DD) method

A received optical signal is made to fall on a PIN diode, which turns it into an electrical form. This detected signal is filtered to reconstruct the original message. The BER for a non-return-to-zero (NRZ) signal can be expressed as [17]:

$$\mathrm{BER} = \frac{1}{2}\mathrm{erfc}\left(\frac{\sqrt{\mathrm{SNR}}}{2\sqrt{2}}\right), \tag{1}$$

where the signal-to-noise ratio (SNR) can be determined as a function of the received optical power.

2.1.2 MZI detection method

DPSK receivers are usually based on interferometry, so a higher-order modulation of DQPSK is configured in the MZI detection method [18]. Figure 2 shows a demodulation of the DQPSK signal, where in-phase (I) and quadrature (Q) signals are filtered in separate sections. The I and Q signals of each section are detected using an MZI with a 45°, −45° phase shift and two-time delay components [19].

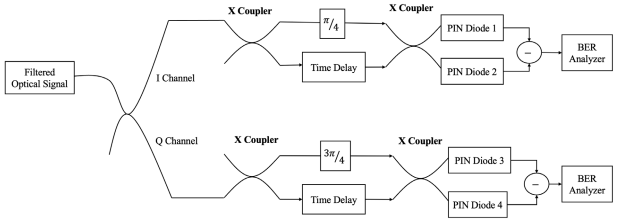

Fig. 2. MZI detection method for a DQPSK signal.

2.1.3 Coherent detection method

Figure 3 provides a layout for the optical coherent detection technique. A filtered optical signal and a 90° phase-shifted LO are coupled and converted to electrical signals using a balanced detection configuration. This setup removes unnecessary noise and provides the I and Q channels to the digital signal processing (DSP) unit [20].

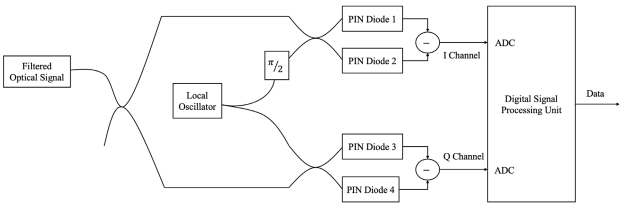

Fig. 3. Coherent detection method along with a DSP module.

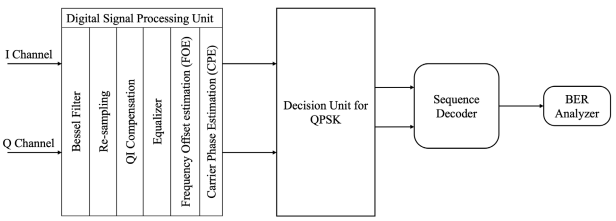

Fig. 4. Stages in the DSP module.

The received electrical signal has timing, phase, and frequency errors which are repaired in the DSP module shown in Fig. 4. At first, the shape of the signal has to be corrected to remove band noise using a 3rd order Bessel filter. Based on interpolation, re-sampling is carried out in the second stage to improve the signal resolution. The imbalance between the amplitude and phase of I and Q channels may occur due to atmospheric effects [21] like scattering and scintillation which can be minimised with the help of the quadrature imbalance compensation stage.

The frequency offset in the received signal is due to an angular mismatch between the filtered signal frequency and the frequency from the LO. This shift in frequency causes inter-carrier interference which can be corrected using frequency offset estimation (FOE). To counteract deteriorating effects caused by laser sources, the carrier phase estimation (CPE) technique is employed [22].

2.2 FSO channel modelling

The optical signal power received would degrade while transmitted over a guideless FSO medium. As the wavelength of optical signals is very small in the order of nm, they tend to scatter, absorb, and refract due to atmospheric particles. Thus, modelling an FSO channel is essential to study the characteristics of the atmosphere. The optical signal power is primarily affected by atmospheric attenuation, geometric loss, and scintillation loss. The optical power received by the FSO system may be mathematically represented in (1) [23]:

$$P_r = P_t \frac{\left(d_r\right)^2}{\left(d_t + \theta R\right)^2} 10^{-\gamma R/10}, \tag{2}$$

where γ is the atmospheric attenuation (dB/km), R is the link range (km), d_r and d_t represent the receiver and transmitter aperture diameter, and θ is the beam divergence (mrad).

2.2.1 Atmospheric loss

In the FSO system, diverse aspects degrade the optical signal power, such as absorption, diffraction, scattering, and reflection of particles in the atmosphere. Optical wavelengths interact with heterogeneous particles like dust, smog, and smoke, as well as weather conditions like fog, rain, and snow, leading to attenuation or scattering (Mie or Rayleigh). Fog is particularly significant as it causes substantial signal loss by reducing visibility near the ground. With respect to the visibility range, the loss incurred due to a foggy climate can be calculated using the Kruse's empirical model, shown in (3):

$$L_{\text{atmo}} = \left(\frac{3.91}{V}\right)\left(\frac{\lambda}{550}\right)^{-\delta}, \tag{3}$$

where δ is the particle size-coefficient, V is the visibility in km, and λ represents the wavelength used in nm.

The authors use Kim's model rather than Kruse's model to accurately predict the particle size which considers visibility less than 1 km [24]. The particle size coefficient varies with the visibility range predicted by Kim's model to anticipate the signal attenuation expressed as [25]:

$$\delta = \begin{cases} 1.6 & V > 50\,\text{km} \\ 1.3 & 6\,\text{km} < V < 50\,\text{km} \\ 0.16V + 0.34 & 1\,\text{km} < V < 6\,\text{km} \\ V - 0.5 & 0.5\,\text{km} < V < 1\,\text{km} \\ 0 & V < 0.5\,\text{km} \end{cases}. \tag{4}$$

2.2.2 Geometric loss

Geometric loss can be a substantial challenge in the FSO communication, especially for long-range links as it limits the achievable link distances and data rates [26]. To optimise the design and maximise the efficiency of the FSO communication system, the transmitter, receiver aperture, and beam divergence should be chosen to achieve the maximum allowable link distance. Beam divergence loss can be given as a ratio of the fraction of power received to transmitted power [27] as per (5):

$$L_{geom} = \frac{P_r}{P_t} = \frac{d_r^2}{(d_t + R\theta)^2}. \tag{5}$$

2.2.3 Scintillation loss

According to the energy cascading theory, increasing wind velocity in the atmosphere generates small, unstable, turbulent eddies. Atmospheric turbulence and its effects can be modelled mathematically by treating fluctuations in parameters like temperature, pressure, and wind velocity as stationary random and isotropic processes [28]. Scintillation loss results from rapid variations in the refractive index (n) caused by stochastic changes in temperature and pressure during signal propagation. The change in refractive index with distance (z) is related to temperature and pressure, represented in (6):

$$n(z) = 1 + 79\left(\frac{P(z)}{T(z)}\right) \times 10^{-6}, \tag{6}$$

where $P(z)$ and $T(z)$ represent the atmospheric pressure in mbar and temperature of the atmosphere in kelvin, respectively. Refractive index structure constant C_n^2 could be simply expressed in terms of temperature index constant C_t^2 in (7):

$$C_n^2 = \left(79\left(\frac{P(z)}{T(z)}\right) \times 10^{-6}\right)^2 C_t^2. \tag{7}$$

Due to irradiance fluctuations caused by the change in refractive index, the scintillation effect degrades the SNR and masks the signal. This scintillation loss can be given for the system in (8):

$$L_{\text{sci}} = 2\sqrt{23.17 C_n^2 k^{7/6} R^{11/6}}. \tag{8}$$

As the fluctuations are considered a random process, they can be mathematically modelled by determining the probability density function (PDF) of the received optical intensity (I). In a recent study, there are several models out of which gamma-gamma distribution is applicable for all regimes (like weak, moderate, and strong). In order to establish the PDF of optical intensity, the gamma-gamma model incorporates the effects of both large-scale eddies which cause refraction and small-scale eddies which cause scattering. The distribution function for the gamma-gamma model can be expressed in (9):

$$p(I)=\frac{2(\alpha\beta)^{(\alpha+\beta)/2}}{\Gamma(\alpha)\Gamma(\beta)}I^{(\alpha+\beta/2)-1}K_{\alpha-\beta}(2\sqrt{\alpha\beta I}),\quad I>0. \tag{9}$$

Here α and β represent the intensity fluctuations of large- and small-scale eddies caused by the scattering process, of order n and $\Gamma(\cdot)$ represent the gamma function, $K_n(\cdot)$ the modified Bessel function of the 2nd order of $(\alpha-\beta)$ [29, 30].

If it is assumed that the optical radiation at the receiver follows a plane wave model, the two parameters α and β describing the probability density function of irradiance fluctuations are given in (10) and (11):

$$\alpha=\left[\exp\left(\frac{0.49\sigma_R^2}{\left(1+1.11\sigma_R^{12/5}\right)^{7/6}}\right)-1\right]^{-1}, \tag{10}$$

$$\beta=\left[\exp\left(\frac{0.51\sigma_R^2}{\left(1+0.69\sigma_R^{12/5}\right)^{5/6}}\right)-1\right]^{-1}, \tag{11}$$

where $\sigma_R^2=1.23C_n^2k^{7/6}R^{11/6}$ shows the Rytov variance, which $k=2\pi/\lambda$ is the propagation constant and R is the link range.

3 System model

In this work, a terrestrial link between two multi-story buildings is considered, establishing an FSO link in a low-visibility environment (960 m). The transmitter section of the system consists of a continuous 1550 nm laser source and a stream of pseudorandom input sequence generated at a data rate of 10 Gbps.

The optical signal travels the FSO link with the modelled features and is detected by photodetectors in the receiver section. The overall simulation has been carried out using OptiSystem software with simulation parameters provided in Table 1. Channel parameters for weak, moderate, and strong scintillation regimes have been displayed in Table 2.

4 Results and discussions

In this section, the FSO system performance has been evaluated with diverse scintillation effects. The optimisation of the achievable link range for each scintillation regime (weak, moderate, and strong) would be determined by the log(BER), which must not exceed an optimal BER limit of $5.6\cdot10^{-5}$

4.1 Direct detection (DD) scheme

With the DD scheme, the maximum possible range of the communication established by an FSO system in a weak regime is 4 km where the optimal BER of $5.6\cdot10^{-5}$ can be reached at a received optical power of −23.35 dBm. As for moderate and strong turbulence regimes, the link range would reach 1.1 km and 90 m, respectively, as atmospheric turbulence would hinder the optical signal.

Figure 5 shows the link range (km) *vs*. log(BER) for the DD scheme. Table 3 represents the performance metrics for the DD scheme with various scintillation regimes. From Table 3, it can be deduced that the strong regime requires huge optical power to detect the deformed signal. As the refractive index structure changes from low to high, the link range decreases and the receiver sensitivity is compromised. Equation (1) indicates that a reduction in SNR leads to the BER degradation.

4.2 MZI detection scheme

For the optimal BER, the link range has been recorded as 3.4 km (weak scintillation), 2.25 km (moderate scintillation), and 200 m (strong scintillation). The BER plot against link range (km) for MZI detection has been plotted in Fig. 6.

Table 4 denotes the performance metrics for the MZI detection scheme with various scintillation regimes. While the MZI scheme demonstrates the improved SNR compared to DD, its practical deployment is constrained by increased system complexity and sensitivity to alignment errors, particularly in high-turbulence environments.

Table 1.
Simulation parameters [31, 32]

Parameter	Values	
Bit rate	10 Gbps	
Sequence length	$2^{16}-1=65535$	
Wavelength used	1550 nm	
Transmitted power	2 dBm	
Linewidth of laser	0.1 MHz	
Fog attenuation	2.5 dB/km	
Transmitter aperture diameter	5 cm	
Receiver aperture diameter	20 cm	
PIN photodetector	Responsivity	1 A/W
	Dark current	10 nA
	Gain	3

Table 2.
Channel parameters [33].

Scintillation regimes	Refractive index structure (C_n^2)
Weak	$5\cdot10^{-18}\ m^{-2/3}$
Moderate	$5\cdot10^{-15}\ m^{-2/3}$
Strong	$5\cdot10^{-13}\ m^{-2/3}$

Table 3.
Performance metrics for DD scheme with various scintillation regimes

	Link range (km)	Received power (dBm)	SNR (dB)	log (BER)
Weak scintillation	4	−23.35	17.41	−4.15
Moderate scintillation	1.1	−5.033	15.84	−4.20
Strong scintillation	0.09	17.31	15.80	−4.12

Table 4.
Performance metrics for MZI detection scheme with various scintillation regimes

	Link range (km)	Received power (dBm)	SNR (dB)	log (BER)
Weak scintillation	3.4	−21.73	38.70	−4.23
Moderate scintillation	2.25	−15.31	15.83	−4.24
Strong scintillation	0.2	9.90	15.27	−4.16

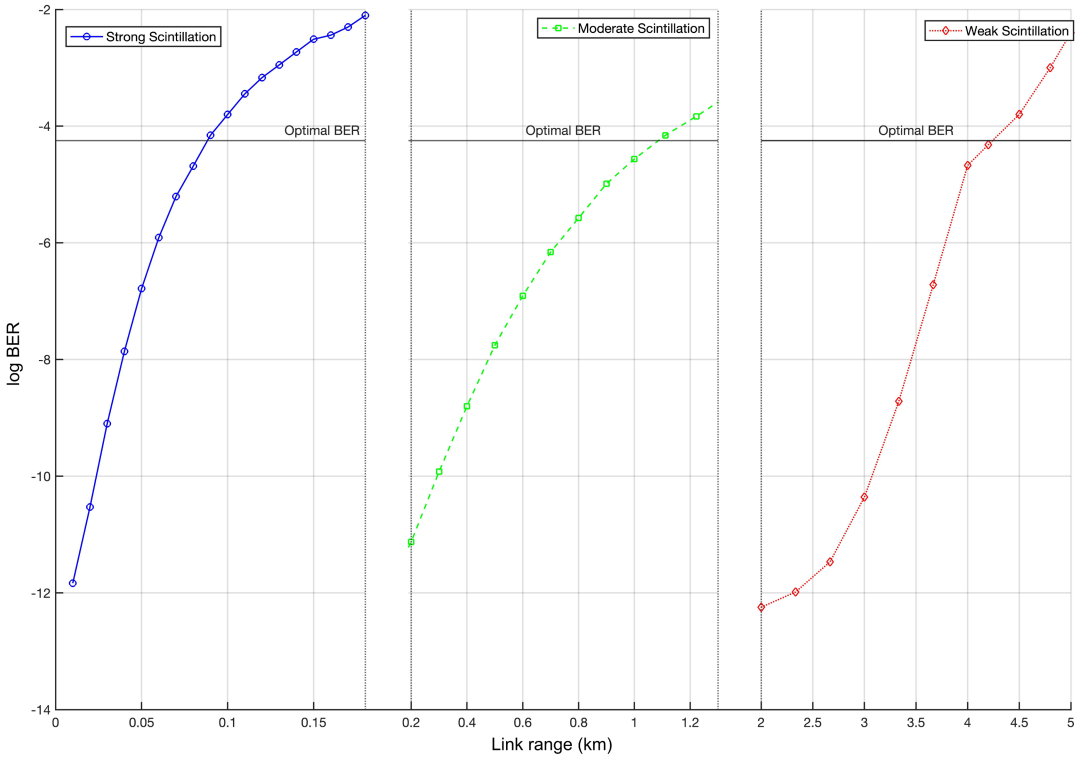

Fig. 5. Log(BER) *vs*. link range (km) under the DD scheme.

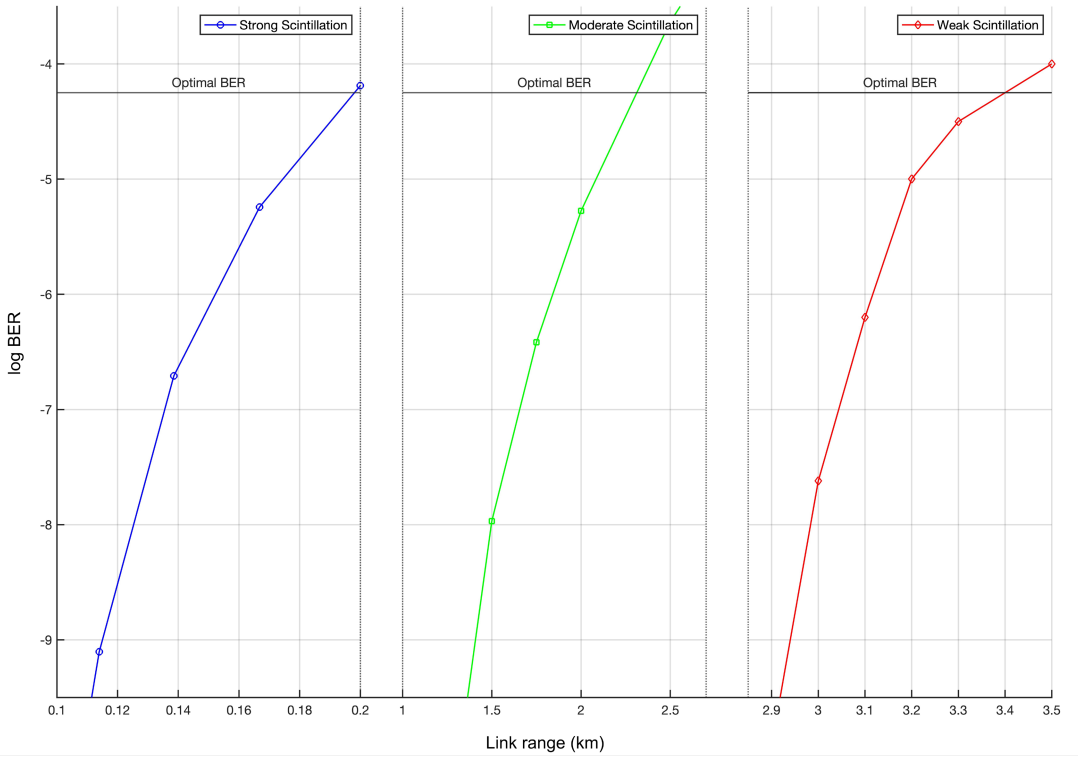

Fig. 6. Log(BER) *vs*. link range (km) under the MZI detection scheme.

4.3 Coherent detection scheme

4.3.1 Optimising maximum link range for FSO system

A coherent detection scheme has been carried out and the maximum feasible link range has been determined as 7.4 km, 6.6 km, and 6.5 km for weak, moderate, and strong turbulence regimes, respectively, as shown in Fig. 7.

In order to achieve a BER of $5.6 \cdot 10^{-5}$ which is the optimal BER limit, the received optical power level must be −40.37 dBm for weak scintillation, −38.8 dBm for moderate scintillation and −36.54 dBm for strong scintillation. The performance metrics for a coherent detection scheme with various scintillation regimes have been tabulated in Table 5.

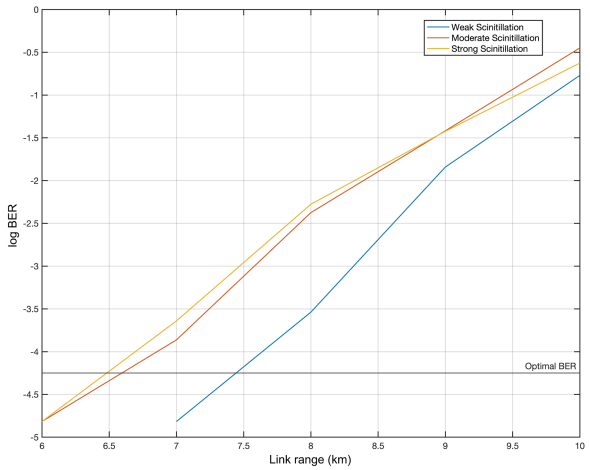

Fig. 7. Log(BER) *vs*. link range (km) under coherent detection scheme.

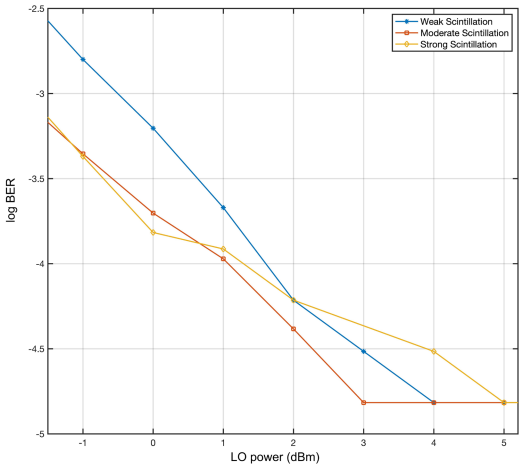

Fig. 8. Log(BER) *vs*. LO power for diverse scintillation effects.

Table 5.
Performance metrics for coherent detection scheme with various scintillation regimes.

	Link range (km)	Received power (dBm)	SNR (dB)	log (BER)
Weak scintillation	7.4	−40.37	17.33	−4.2
Moderate scintillation	6.6	−38.08	10.50	−4.2
Strong scintillation	6.5	−36.54	10.03	−4.2

The scheme incorporates a correction mechanism for the phase difference in the received signal, mitigating scintillation effects. This minimises the required received optical power to achieve the optimal BER. In case of substantial substorms or dusty wind climates, the optical free-space link range is limited because of the scintillation effect. Scintillation reduces the SNR, compromising receiver sensitivity. However, due to DSP capabilities, coherent detection partially corrects signal distortions. Thus, deploying a coherent detection scheme for such harsh weather conditions is recommended as it would minimise scintillation effect and effectively enhance the link range.

4.3.2 Optimising LO power

In the FSO system, diverse aspects degrade the optical signal power, such as absorption and diffraction. Figure 8 illustrates the log(BER) against the LO power (dBm) for three different scintillation regimes.

Under weak scintillation conditions, the BER is significantly lower and reaches below the forward error correction (FEC) limit with a relatively low LO power (~2 dBm). For moderate and strong scintillation regimes, higher LO power (3–5 dBm) is required to achieve a similar BER performance. The results emphasize the importance of LO power in mitigating scintillation effects and enhancing the receiver sensitivity.

The optimisation of LO power in coherent detection systems plays a crucial role in maintaining reliable communication under varying scintillation conditions, particularly in strong turbulence. The results indicate that higher LO power effectively mitigates scintillation-induced distortions over longer distances. Table 6 summarises the comprehensive analysis of the existing works with the proposed scheme in terms of laser power (dBm), data rate (Gbps), and maximum possible link range (km). Notably, the proposed work uses less transmitted laser power to achieve a longer distance than other existing works.

DD is the most cost-efficient and least complex option, making it suitable for weak scintillation regimes. However, its performance is limited in challenging conditions. MZI detection, while offering a moderate performance, is more complex to implement and is better suited for moderate scintillation regimes.

Table 6.
Performance comparison of the proposed systems with reported works.

Ref.	Methods	Data rate (Gbps)	Laser power (dBm)	Weather conditions	Detection schemes	Maximum link range (km)
[33]	Dual polarized QPSK modulation with spatial diversity in FSO system	10	4	Light fog + No scintillation	Coherent	1.3
[34]	SS-WDM-NRZ-based FSO link	1.56	25	Light fog + No scintillation	Direct	3.8
[35]	WDM-FSO link with DPSK scheme	10	10	Light fog + Weak scintillation	MZI	3
[36]	4-QAM-based OFDM-Ro-FSO link	10	16	Light fog + No scintillation	Coherent	2.2
Proposed work	OOK, DQPSK, and QPSK modulation with scintillation effects	10	2	Light fog + Weak scintillation	Direct	4
		10	2	Light fog + Weak scintillation	MZI	3.4
		10	2	Light fog + Weak scintillation	Coherent	7.4

Coherent detection provides the best performance, especially in strong scintillation environments. Despite its advantages, coherent detection has practical limitations including the need for highly stable LOs, complex synchronization mechanisms, and precise alignment requirements which can increase the overall system cost. Since a highly stable LO source may reduce feasibility in low-cost applications, optimising laser power is essential. Each detection scheme has its strengths and is best suited for specific atmospheric conditions and performance requirements.

5 Conclusions

The performance of a 10 Gbps FSO transmission link using DD, MZI detection, and coherent detection schemes has been evaluated. DD and MZI detection schemes offer reasonable alternatives in less challenging atmospheric conditions, with DD being cost-efficient and less-complex and MZI detection providing moderate performance in moderate scintillation environments. Coherent detection achieves maximum feasible ranges of 7.4 km, 6.6 km, and 6.5 km under weak, moderate, and strong scintillation, respectively, and is significantly enhanced by optimising LO power, improving system reliability under strong turbulence. A reliable FSO communication link could be established using a coherent detection with optimised LO power as a practical solution for extending FSO communication reliability in real-world applications, such as 5G backhaul networks, satellite-to-ground links, and high-speed optical data relays. Future work explores the integration of adaptive optics and advanced modulation formats to further mitigate the scintillation effects and enhance link performance in next-generation optical communication systems.

Authors' statement

Conceptualisation and design of this study, original writing and original draft, analysis of results, writing, review and editing, S.V.M.S.; collection and data analysis, K.P.; review and editing and analysis of the results, K.P. and P.P.; supervision, P.P.; critical revision of the article, P.P. and S.A.

Acknowledgements

The authors would like to thank the financial support from Anna University – Anna Research Fellowship (ARF) (Lr. No.: CFR/ARF-Jan2023/AR1).

References

[1] Kadem, K. H. & Mohammed, M. F. Enhancement security and camouflage for free-space optical communication system reliance on switching between structured light beams. *Opto-Electron. Rev.* **32**, e152684 (2024). https://doi.org/10.24425/opelre.2024.152684

[2] Song, S., Wu, J., Liu, Y. & Guo. L. A novel low-complexity high-order DPSK system with constellation reconstruction for FSO communication. *IEEE Wirel. Commun. Lett.* **11**, 2031–2035 (2022). https://doi.org/10.1109/LWC.2022.3191659

[3] Krishna, K. M., Madhan, M. G. & Ashok. P. Performance predictions of VCSEL based cascaded fiber-FSO RoF system for 5G applications. *Optik* **257**, 168740 (2022). https://doi.org/10.1016/j.ijleo.2022.168740

[4] Prakash, P., Kasthuri, P., Ganeshmadhan, M. & Prakash, A. Simulations of mode division multiplexed free space optics with photonicstraversal filter using multi-mode fiber. *Inf. MIDEM* **51**, 207–213 (2021). https://doi.org/10.33180/infmidem2021.401

[5] Anuranjana, S., Kaur, R., Goyal, R. & Chaudhary, S. 1000 Gbps MDM-WDM FSO link employing DP-QPSK modulation scheme under the effect of fog. *Optik* **257**, 168809 (2022). https://doi.org/10.1016/j.ijleo.2022.168809

[6] Mahmood, A. S. An approach to investigating the feasibility of free-space optical communication technology deployment under scintillation effects. *Opto-Electron. Rev.* **31**, e147037 (2023). https://doi.org/10.24425/opelre.2023.147037

[7] Gao, S., Dang, A. & Guo, H. Performance of Wireless Optical Communication Systems Using DPSK Modulation. in *2009 11th International Conference on Advanced Communication Technology* 1793–1796 (IEEE, 2009).

[8] Wang, Z., Zhong, W.-D., Fu, S. & Lin, C. Performance comparison of different modulation formats over free-space optical (FSO) turbulence links with space diversity reception technique. *IEEE Photon. J.* **1**, 277–285 (2009) https://doi.org/10.1109/JPHOT.2009.2039015

[9] Jaworski, M. Optical Modulation Formats for High-Speed DWDM Systems. in *Proceedings of 2003 5th International Conference on Transparent Optical Networks* 162–165 (IEEE, 2003). https://doi.org/10.1109/ICTON.2003.1263171

[10] Padhy, J. B. & Patnaik, B. Multiplexed free-space optical system design using Manchester coding. *Optik* **174**, 266–273 (2018). https://doi.org/10.1016/j.ijleo.2018.07.140

[11] Xie, G., Dang, A. & Guo, H. Performance Analysis of Free Space Optical Communication Based on DPSK Modulation. in *Lasers Sources and Related Photonic Devices OSA Technical Digest Series (CD)* LSMC5 (Optica Publishing Group, 2010). https://opg.optica.org/abstract.cfm?URI=LSC-2010-LSMC5

[12] Nasu, Y. *et al*. Polarization Insensitive MZI-Based DQPSK Demodulator with Asymmetric Half-Wave Plate Configuration. in *Optical Fiber Communication Conference/National Fiber Optic Engineers Conference* OThE5 (Optica Publishing Group, 2008).

[13] Ho, K.-P. *Phase-Modulated Optical Communication Systems.* (Springer-Verlag, 2005).

[14] Patnaik, B. & Sahu, P. K. Novel QPSK Modulation for DWDM Free Space Optical Communication System. in *2012 Wireless Advanced (WiAd)* 170–175 (IEEE, 2012). https://doi.org/10.1109/WiAd.2012.6296557

[15] Palanisamy, A. R. *et al*. 10 Gbps CPFSK FSO system under various adverse atmospheric conditions: performance analysis. *Opt. Quant. Electron.* **55**, 911 (2023). https://doi.org/10.1007/s11082-023-05169-x

[16] Patnaik, B. & Sahu, P. K. Inter-satellite optical wireless communication system design and simulation. *IET Commun.* **6**, 2561–2567 (2012). https://doi.org/10.1049/iet-com.2012.0044

[17] Mandal, S. K., Bera, B. & Dutta, G. G. Free Space Optical (FSO) Communication Link Design under Adverse Weather Condition. in *2020 International Conference on Computer, Electrical & Communication Engineering (ICCECE)* 1–6 (IEEE, 2020). https://doi.org/10.1109/iccece48148.2020.9223023

[18] Lim, H.-C. *et al*. Performance analysis of DPSK optical communication for LEO-to-ground relay link via a GEO Satellite. *J. Astron. Space Sci.* **37**, 11–18 (2020). https://doi.org/10.5140/jass.2020.37.1.11

[19] Selvendran, S. & Sivanantharaja, A. Analysis of four wave mixing under different all optical modulation formats. *J. Nonlinear Opt. Phys.* **22**, 1350034 (2013). https://doi.org/10.1142/s0218635135003343.

[20] Singh, H. Design and analysis of high-speed free space optical (FSO) communication system for supporting fifth generation (5G) data services in diverse geographical locations of India. *IEEE Photon. J.* **13**, 1–12 (2021). https://doi.org/10.1109/JPHOT.2021.3113650

[21] Faruk, M. S. & Kikuchi, K. Compensation for in-phase/quadrature imbalance in coherent-receiver front end for optical quadrature amplitude modulation. *IEEE Photon. J.* **5**, 7800110 (2013). https://doi.org/10.1109/JPHOT.2013.2251872

[22] Patel, D. K. & Mandloi, A. S. Data reliability enhancement using RS coded DP-16-QAM based FSO system under different weather conditions. *Opt. Quantum Electron.* **53**, 228 (2021). https://doi.org/10.1007/s11082-021-02989-7

[23] Ali, M. A. A., Adnan, S. A. & Al-Saeedi, S. A. Transporting 8 × 10 Gbps WDM Ro-FSO under various weather conditions. *J. Opt. Commun.* **41**, 99–105 (2017). https://doi.org/10.1515/joc-2017-0140

[24] Sovmaja Vathsan, M. S., Kasthuri, P., Poornachari, P. & Sasistnradevi, A. Analysis of atmospheric attenuation of a FSO-WDM system for long-range communication. *J. Opt. Commun.* **45**, 2059–2066 (2023). https://doi.org/10.1515/joc-2023-0157

[25] Kaushal, H., Jain, V. K. & Kar, S. *Free Space Optical Communication*. (Springer, 2017).

[26] Kaur, S. Analysis of inter-satellite free-space optical link performance considering different system parameters. *Opto-Electron. Rev.* **27**, 10–13 (2019). https://doi.org/10.1016/j.opelre.2018.11.002

[27] Pate, D. K., Mandloi, A., Srivastava, V. & Tripathi, A. Investigation of RS-Code DP-QPSK enabled FSO Communication Link under various Atmospheric Conditions. in *2022 13th International Symposium on Communication Systems, Networks and Digital Signal Processing (CSNDSP)* 223–228 (IEEE, 2022). https://doi.org/10.1109/CSNDSP54353.2022.9908011

[28] Handura, M. R., Ndjavera, K. M., Nyirenda, C. N. & Olwal, T. O. Determining the feasibility of free space optical communication in Namibia. *Opt. Commun.* **366**, 425–430 (2016). https://doi.org/10.1016/j.optcom.2015.12.057

[29] El-Nahal, F., Xu, T., AlQahtani, D. & Leeson, M. A bidirectional wavelength division multiplexed (WDM) free space optical communication (FSO) system for deployment in data center networks (DCNs). *Sensors* **22**, 9703 (2022). https://doi.org/10.3390/s22249703

[30] Singh, H. & Mittal, N. Link budget analysis of free space optical communication link for atmospheric conditions of India. *Mater. Today: Proc.* **48**, 1064–1069 (2022). https://doi.org/10.1016/j.matpr.2021.07.188

[31] Liang, J., Chaudhry, A. U., Erdogan, E. & Yanikomeroglu, H. Link Budget Analysis for Free-Space Optical Satellite Networks. in *2022 IEEE 23rd International Symposium on a World of Wireless, Mobile and Multimedia Networks (WoWMoM)* 471–476 (IEEE, 2022). https://doi.org/10.1109/WoWMoM54355.2022.00073

[32] Li, X. *et al*. Performance improvement of coherent free-space optical communication with quadrature phase-shift keying modulation using digital phase estimation. *Appl. Opt*. **56**, 4695–4701 (2017). https://doi.org/10.1364/AO.56.004695

[33] Rajput, S. J. & Acharya, Y. B. Performance analysis of 25 Gbps DP-QPSK based CO-OFDM-FSO link incorporating spatial diversity under climate conditions and atmospheric turbulence. *Prog. Electromagn. Res. C* **133**, 151–165 (2023). https://doi.org/10.2528/pierc23031505

[34] Prabu, K., Charanya, S., Jain, M. & Guha, D. BER analysis of SS-WDM based FSO system for Vellore weather conditions. *Opt. Commun.* **403**, 73–80 (2017). https://doi.org/10.1016/j.optcom.2017.07.012

[35] Badar, N., Jha, R. K. & Towfeeq, I. Performance analysis of an 80 (8×10) Gbps RZ-DPSK based WDM-FSO system under combined effects of various weather conditions and atmospheric turbulence induced fading employing Gamma–Gamma fading model. *Opt. Quantum Electron.* **50**, 44 (2018). https://doi.org/10.1007/s11082-017-1306-y

[36] Grover, A. & Sheetal, A. Improved performance investigation of 10 Gb/s–10 GHz 4-QAM based OFDM-Ro-FSO transmission link. *J. Opt. Commun.* **44**, 1141–1148 (2019). https://doi.org/10.1515/joc-2019-0223